Layer-by-layer assembly of food-grade alginate/chitosan nanolaminates: formation and physicochemical characterization

Authors:

Acevedo-Fani, Alejandra

Salvia-Trujillo, Laura

Soliva-Fortuny, Robert

Martín-Belloso, Olga* (author to whom correspondence should be addressed)

Affiliations:

Department of Food Technology.

University of Lleida - Agrotecnio Centre.

Av. Alcalde Rovira Roure 191.

25198, Lleida, Spain

Information of the corresponding author:

E-mail: omartin@tecal.udl.es

Telephone and fax number: +34 973 702593 / +34 673 328 227

ABSTRACT

The alternate deposition of oppositely charged materials (layer-by-layer technique) is an effective approach to functionalize materials. Biopolymer-based nanolaminates obtained by the layer-by-layer technique can also be used to change the surface properties of food products or food contact materials. However, the final properties of nanolaminates may be affected by the conditions of the adsorbing solutions. The objective of this study was to form and characterize the physicochemical properties of nanolaminates assembled from alginate and chitosan solutions. The effect of pH, ionic strength and polysaccharide concentration on the properties of the absorbing solutions was also evaluated. The ζ-potential, viscosity and whiteness index of the solutions were assessed before the assembly. Alginate/chitosan nanolaminates were characterized in terms of UV-visible spectroscopy, surface ζ-potential, contact angle, DSC analysis and SEM. The absorbance increased as a function of the number of polysaccharide layers on the substrate, suggesting an increase in the mass adsorbed. The surface ζ-potential of nanolaminates changed depending on the last polysaccharide deposited. Alginate layers were negatively charged, whereas chitosan layers were positively charged. Contact angles obtained in alginate layers were ≈ 10º, being mostly hydrophilic. Chitosan layers showed higher contact angle values (80º), indicating a more hydrophobic behavior. Microscopic examinations revealed the presence densely packed structures that corresponded to alginate/chitosan nanolaminates, having an estimated thickness of 700 nm. The results obtained in this work lay the basis for the rational design of polysaccharide-based nanolaminates in the food sector.

Keywords: alginate; chitosan; layer-by-layer; nanolaminates, food-grade coatings and films

1. Introduction

Nowadays, the use of nanomaterials in the food field is becoming rather important since it can offer remarkable prospects to design innovative products and applications in many industrial sectors, ranging from food processing, novel foods, food additives and food contact materials [1]. In particular, nanolaminates have been recently proposed as a potential strategy to modify the surface properties of either food contact materials (e.g. plastics films, paper, and aluminum) or foodstuffs (e.g. fruits, vegetables, meats, and candies). These modifications can improve the material properties.

Nanolaminates are defined as thin coatings formed on a substrate by the sequential deposition of at least two layers of different materials, wherein the typical thickness is less than 100 nm per layer. The final thickness depends on the number of layers deposited [2]. These nanolaminate structures are obtained by the well-known layer-by-layer (LbL) assembly technique, which consists on the alternate adsorption of species (normally, polyelectrolytes) using different chemical interactions. Electrostatic bonding, hydrogen bonding, hydrophobic interactions, charge-transfer interactions, covalent bonding are among the most commonly explored [3].

So far, the most common approach used to produce nanolaminates is the electrostatic interactions between oppositely charged species [3]. The LbL method has been widely explored for several applications in different science fields (e.g. material science, pharmacology or biomedicine) due to its simplicity, high adaptability and low-cost [4]. In food science, the LbL method is mainly utilized to create interfacial coatings around spherical templates in colloidal systems (e.g. emulsions, liposomes or capsules). It has been found that interfacial nanolaminate coatings increase the stability of colloidal dispersions under stressing conditions including pH, temperature or ionic strength, or may modulate lipid digestion and release of entrapped bioactive compounds [5,6]. Other authors have proved that biopolymer-based nanolaminates can be created on food surfaces, such as fruits and vegetables, delaying the typical deleterious reactions that lead to food spoilage [7]. The major advantage of this procedure is the possibility to fine-tune the characteristics of nanolaminates by simply controlling the processing parameters, such as polyelectrolyte type, molecular weight, charge density, the conditions of adsorbing solutions (pH, ionic strength, polyelectrolyte concentration, and temperature), adsorption and rinse times, drying between layers, number of layers deposited and washing steps, or the terminal layer [3].

Polysaccharides have been playing an important role within the food industry, working as additives to improve, modify and stabilize food texture properties, but also to produce edible food packaging systems (e.g. films and

coatings for solid foods), and more recently, for the nanoencapsulation of food ingredients. Polysaccharides are biodegradable, present good gas barrier properties and high compatibility with foods [8]. Nevertheless, when functional groups with charged moieties are present in the backbone, polysaccharides behave as polyelectrolytes, which enable their use as building blocks for assembling food-grade nanolaminates by electrostatic interactions [9]. For instance, alginate is a natural linear copolymer extracted from marine brown algae, consisting of 1-4 linked β-D-mannuronic acid and α-L-guluronic acid. The negative charge of alginate is provided by ionized carboxyl functional groups (COO^-) of mannuronic and guluronic acid monomers whose dissociation constants (pK_a) are 3.3 and 3.6, respectively [10].

Chitosan, a deacetylated form of chitin, is a naturally-occurring polysaccharide found in the exoskeleton of crustaceans and fungi. Chitosan is formed by *N*-acetylglucosamine and glucosamine residues, being soluble in acidic media because of the protonation of $-NH_2$ groups of D-glucosamine residues. Then, the positive charge of chitosan is given by the protonated amine groups (NH_3^+), with a pK_a around ≈ 6.3 [11]. On the other hand, polyethylene terephthalate (PET) has been extensively used as a versatile food contact material [12]. PET has also been reported as a suitable substrate to produce polysaccharide-based nanolaminates [13], since its properties are well described, allowing to characterize the physical and chemical characteristics of nanolaminates. Quartz is another type of substrate commonly used for monitoring the layer-by-layer build-up when using spectrophotometric techniques, such as UV-visible spectroscopy [14].

The conditions of preparation of the absorbing solutions, including the pH, ionic strength or concentration may affect the layer-by-layer assembly using weak polyelectrolytes, such as alginate and chitosan [9]. The effect that changes in the pH and ionic strength of deposition solutions have on the chitosan/heparin nanolaminates properties was previously investigated [15]. In this study, the growth of layer-by-layer assemblies was highly dependent on the solution conditions increasing the mass absorption by an increase in the ionic strength at a fixed pH, or increasing the pH at a constant ionic strength. Therefore, knowledge of polysaccharides behavior is crucial to determine adequate experimental conditions for designing nanolaminates. The main objective of this work was to form and characterize food-grade nanolaminates by the layer-by-layer technique, as well as assess the effect on the conditions of preparation on the electrical charge and physical stability of polysaccharide solutions. This was necessary to find the suitable experimental conditions to prepare the nanolaminates.

2. Materials and methods

2.1. Materials

Food grade sodium alginate (MANUCOL® DH) was purchased from FMC Biopolymers (Scotland, UK). Chitosan (High molecular weight ≈310000-375000 Da; deacetylate degree: > 75 %) was acquired from Sigma-Aldrich (Steinheim, Germany). Lactic acid (88 – 90 %) and sodium hydroxide were obtained from Sharlau Chemie (Barcelona, Spain). Sodium chloride (POCH, Poland) was purchased from Afora (Barcelona, Spain). Quartz slides (Suprasil® 300) and polyethylene terephthalate (PET) sheets were obtained from Hellma Analytics (Müllhein, Germany) and Isovolta (Barcelona, Spain), respectively. All polysaccharide solutions were prepared in deionized water obtained from a Milli-Q filtration system (18.2 mΩ, Merck Millipore, Madrid, Spain).

2.2. Preparation of polysaccharide solutions

2.2.1. Effect of pH

Powdered alginate and chitosan solutions were prepared at different concentrations (0.1- 1% w/v) by dispersing them into water or lactic acid solution (1% v/v), respectively, under continuous stirring overnight. Lactic acid, an organic acid widely used in the food industry, is used as chitosan solvent providing proper acidic conditions for its complete dissolution. Then, both solutions were adjusted to pH 3 to 11, using either lactic acid (1 M) or NaOH (1 M) solutions. Finally, polysaccharide solutions were transferred into plastic bottles, closed and stored at room temperature (≈ 25º C) for the subsequent analysis as described in section 2.3.

2.2.2. Effect of ionic strength

Alginate and chitosan were dissolved in water and lactic acid (1% v/v) respectively, at different concentrations (0.1 – 1% w/v). Then, different amounts of sodium chloride (NaCl) were added to polysaccharide solutions under continuous stirring until complete dissolution to obtain concentrations from 0.1 M to 0.5 M. Finally, alginate and chitosan were adjusted to pH 5 and 4, respectively. Solutions were transferred into plastic bottles, closed and stored at room temperature (≈ 25º C) for the subsequent analysis as described in section 2.3.

2.3. Polysaccharide solutions properties

2.3.1. ζ-Potential

Changes in the electrical charge of polysaccharide chains in aqueous solutions were performed with a laser diffractometer (Zetasizer Nano ZS, Malvern Instruments, Worcestershire, UK) operating at 633 nm. The ζ-potential was measured by Laser Doppler Velocimetry (LDV) and calculated by the Smoluchowski approximation. Alginate and chitosan solutions without previous dilution were placed into a clear plastic zeta cell (DTS 1061, Malvern, UK) to carry out measurements. Two independent runs with three repetitions of each sample were performed. The measurement consists on placing two gold paddles inside the liquid that then vibrates, stimulated by an electromagnetic drive at a constant amplitude. The shear waves imparted to the liquid are damped at a rate that is a function of the viscosity of the liquid. The power required to maintain a constant amplitude is proportional to the viscosity of the fluid, and is measured and transformed to a value of viscosity.

2.3.2. Viscosity measurements

The viscosity of polysaccharide solutions was analyzed in a sine-wave vibro viscometer (SV-10, A&D Company, Tokyo, Japan), with a range from 0.3 mPa.s to 10000 mPa.s operating at 30 Hz and a constant amplitude (less than 1 mm). Alginate and chitosan solutions were analyzed at ≈ 25ºC and this parameter was monitored by the same device. Two independent runs with four repetitions of each sample were performed. The instrument was calibrated with distilled water as a standard solution.

2.3.3. Whiteness index

The optical properties of polysaccharide solutions were analyzed using a colorimeter Minolta CR-400, working with an illuminant D_{65} and 10° observer angle (Konica Minolta Sensing Inc., Osaka, Japan). A crystal flat-faced cuvette was filled with the solutions and put in the measuring device to obtain the CIE Lab parameters. Measurements were performed at room temperature (≈ 25 ºC). The colorimeter was calibrated with a white standard plate (Y = 94, x = 0.3158, y = 0.3222) prior to analyses. Whiteness index (WI) of alginate and chitosan solutions was calculated with the following equation [16]:

$$WI = 100 - \sqrt{(100 - L^*)^2 + \left(a^{*2} + b^{*2}\right)} \qquad \textbf{Eq. (1)}$$

Two independent runs with four repetitions were performed for each sample.

2.4. Layer-by-layer assembly procedure

Alginate/chitosan nanolaminates were formed on quartz slides and PET sheets (2 x 6 cm). As a previous step, both substrates were cleaned and grafted with amino groups to provide an initial positive charge to the substrates' surface. The procedure for substrate pre-treatment was described in great detail in a previous work of our group [17]. Briefly, quartz slides were cleaned in Hellmanex® solution (2%) for 2 h. Then, substrates were immersed in an APTS solution (1% v/v) for 30 min to induce grafting of amino groups, and this was followed by a rinse step with deionized water. The PET sheets were cleaned using a water/propanol solution 50:50, for 3 h. Cleaned sheets were immersed in 1,6-hexanodiamine/methanol solution 1 M, at 50 ºC and 4 h. Afterwards, substrates were washed with methanol and dried for 12 h. Finally, PET substrates were positively charged by submerging them into an HCl 0.1 M solution for 3 h at room temperature.

Both quartz and PET slides (positively charged) were submerged in alginate solutions (negatively charged) at pH 5 for 20 minutes, followed by two rinse steps in water at pH 5 for 5 minutes. Afterwards, substrates were immersed in chitosan solutions (positively charged) at pH 4 for 20 minutes, and two rinse steps with water at pH 4 for 5 min were carried out. The alginate and chitosan adsorption cycles were repeated in order to produce 10-layer nanolaminates. Finally, these assemblies were dried using gas nitrogen when the layer-by-layer process was ended.

2.5. Characterization of nanolaminates

2.5.1. Buildup

The assembly process of alginate and chitosan layers on quartz slides was monitored by measuring the increase in absorbance of the substrate after an adsorption step. Dried substrates containing different number of layers were analyzed in a UV-visible-NIR spectrometer (V-670, Jasco Corporation, Tokyo, Japan), using a film holder accessory (FLH-740, Jasco Corporation, Tokyo, Japan). Absorbance spectra were recorded from 190 nm to 700 nm.

2.5.2. Surface ζ-potential

The surface ζ-potential of alginate and chitosan layers after each adsorption was measured in a laser diffractometer Zetasizer NanoZS (Malvern Instruments Ltd, Worcestershire, UK) equipped with a surface ζ-potential cell unit (ZEN1020) specially designed to measure the ζ-potential in planar surfaces. Rectangles (5 x 4 mm) of alginate/chitosan nanolaminates assembled on PET sheets were attached to a sample holder with glue (Araldite®)

and then dried for 12 h. Sample holders with samples were placed between two electrodes into the surface ζ-potential cell unit using a screwdriver. Then, the cell unit was put into a disposable polystyrene cuvette (DTS0012, Malvern Instruments) previously filled with 1 mL of a suspension containing negative tracer particles, (polystyrene latex particles in buffer solution pH 9, DTS1235, Malvern instruments) or positive tracer particles (quaternary ammonium salts from fragrance-free fabric conditioner solutions in a ratio of 1:100). The surface ζ-potential of alginate layers was analyzed using negative tracer particles, whereas the surface charge of chitosan layers was assessed with positive tracer particles to avoid particle adsorption. The apparent mobility of the tracer particles was determined at five vertical distances from the sample surface (125, 250, 375, 500 and 625 microns). Five measurements were performed in each distance point. The ζ-potential of tracer particles was measured at 1500 microns from the sample surface. The surface ζ-potential of alginate and chitosan layers was calculated by extrapolating the 'zero' distance from the ζ-potential vs displacement graphs using the Zetasizer Software version 7.11 (Malvern Instruments). Four readings were carried out per sample.

2.5.3. Wetting properties

The contact angle measurements of nanolaminates assembled on PET sheets were measured after each layer formation, using a goniometer (DSA25, Krüss GmbH, Hamburg, Germany). The water contact angle was carried out with the sessile drop method, in which a deionized water drop (1 µL) is created at the tip of the syringe and then placed onto the nanolaminate surface at room temperature. Immediately, the contact angle formed by the water drop onto the surface was recorded using the Drop Shape Analysis System software (Krüss GmbH) and calculated through the Young-Laplace fit. Six measurements were performed for each sample.

2.5.4. Thermal properties

The influence of a nanolaminate coating on the thermal properties of PET sheets (used as substrate) was examined by Differential Scanning Calorimetry (DSC) using a DSC822e system (Mettler Toledo, Barcelona, Spain). PET sheets and PET coated by alginate/chitosan nanolaminates were studied in a temperature range of 0-400 ºC at a scanning rate of 10 ºC/min under an atmosphere of inert nitrogen. Samples of ≈ 5 mg were put into aluminum pans (1/8 ME-51119872 aluminum crucibles 100 µl without pin) for analysis. An empty aluminum pan was used as reference and measurements were performed in duplicate. Thermograms were analyzed by the StartE v.11 software (Mettler Toledo). Thermal properties such as the glass transition temperature (T_g), the melting temperature (T_m) and the enthalpy of melting (ΔH_m) were determined from the thermograms. The enthalpy of

meting was calculated by integrating the peak area, drawing a baseline from the onset to the end of the thermal transition.

2.5.5. SEM imaging

SEM micrographs of nanolaminates assembled on PET sheets were obtained with a Scanning Electron Microscope (J-6510, JEOL Ltd, Tokyo, Japan). PET sheets coated by 10-layer nanolaminates were placed onto aluminum stubs, coated with carbon and metalized with evaporated gold in a sputter coater (SCD050, Balzers Union AG, Liechtenstein). Treated samples were analyzed by SEM with an acceleration voltage of 5 kV.

2.6. Statistics

Data obtained from measuring the properties of alginate and chitosan solutions were analyzed by two-way ANOVA using the Statgraphics Plus 5.1 statistical package (Statistical Graphics Co., Rockville, MD, EE.UU). Fisher's least significant difference (LSD) procedure was used to determine differences among means at a 5% significance level. Data obtained from the nanolaminates characterization was reported as the average ± standard deviation of the repetitions.

3. Results and discussion

Initially, polysaccharide solutions used to prepare alginate/chitosan nanolaminates were characterized in terms of electrical charge, viscosity and optical properties varying the solvent composition (pH, ionic strength) and polysaccharide concentration. Preliminary analysis of the behavior of polysaccharides was used to set out the experimental parameters for the layer-by-layer assembly of nanolaminates.

3.1. Changes in the electrical charge of polysaccharides

The ζ-potential of alginate and chitosan molecules was evaluated as a function of pH, ionic strength and polysaccharide concentration of the solution (Fig. 1). Alginate solutions had rather negative ζ-potentials (< -70 mV) from pH 5 to 11, but became less negative at pH 3 (≈ -40 mV). The decrease in the magnitude of the electrical charge at pH 3 was attributed to the protonation of the carboxyl groups of alginate ($pK_a \approx 3.65$) [18]. The polysaccharide concentration also affected the electrical charge of alginate chains. Higher alginate concentration resulted in more negative ζ-potential values. This effect could be explained by the presence of a greater number of protonated carboxyl groups available to provide an electrical charge in the colloidal system.

The electrical charge of chitosan solutions was strongly positive in acidic conditions. The greatest ζ-potential values at pH 3 (45 mV, 0.1 %). Nevertheless, an increase in the pH to more alkaline conditions decreased the electrical charge of chitosan molecules. This indicated that chitosan chains were less ionized. Chitosan solutions with pH values above 7 or with 1% w/w of concentration could not be analyzed. Polysaccharides were insoluble, presenting clumps of great size that could not be placed in the measurement cell. These results are in good agreement with those reported by other authors, where the increase in pH of polysaccharide solutions, including alginate and chitosan, led to a decrease of the magnitude of the positive ζ-potential [19].

On the other hand, the presence of NaCl in the solution decreased the magnitude of ζ-potential values for both polysaccharides (Fig. 1B). For instance, the ζ-potentials of alginate and chitosan without NaCl were -83 mV and 72 mV at 0.5 %, respectively. At 0.2 M NaCl, the magnitude of the ζ-potential decreased to -37 mV and 33 mV in alginate and chitosan solutions, respectively. The effect of the ionic strength on the ζ-potential was less pronounced at higher NaCl concentrations (0.5 M). Previous studies demonstrated a reduction of the net charge in alginate and chitosan solutions as the ionic strength increased [20]. This predictable behavior of polysaccharides may be governed by a compression of the electrical double layer due to the electrostatic interactions with Na^+ and Cl^- ions dispersed in the solvent [21].

3.2. Changes in the viscosity of polysaccharide solutions

The conformation and chain dimensions of polyelectrolytes in the adsorbing solutions has a strong influence on the growth behavior, structure and properties of the resulting nanolaminates [22]. The viscosity of the solution, may give valuable information about the conformations of macromolecules in different conditions. Therefore, the effect of pH, ionic strength and polysaccharide concentration on the viscosity of adsorbing solutions was investigated (Fig. 2).

The viscosity increased with the concentration of polysaccharide, due to the greater entanglement of chains and an increase of the effective volume fraction of the disperse phase [23]. On the other hand, with the exception of pH 3, the viscosity of alginate solutions was not affected by the pH. A decrease in viscosity was observed in alginate solutions at pH 3 (Fig. 2A). This is reasonable since the ζ-potential values of alginate solutions were weaker at this pH value. Hence, alginate chains could have adopted coiled conformations induced by the protonation of the carboxylic acid groups (COO^-) thereby reducing their hydrodynamic size and solvation. It has been stated that linear and stiff polymers (fully charged polyelectrolytes) have a larger hydrodynamic size than

highly flexible polymers (weakly charged polyelectrolytes) of the same molecular mass, resulting in a higher viscosity of the solution [24].

In the case of chitosan solutions, an increase in the pH led to a decrease in viscosity. This effect was less pronounced at low polysaccharide concentrations (Fig. 2A). It is worth mentioning that chitosan solutions at pH above 7 presented insoluble clumps, indicating that solutions were not physically stable within this pH range (>7). This behavior is understandable since these pH values are closer to the pK_a of the glucosamine residues in chitosan (≈ 6-6.5), where most of the amino groups were not ionized [11]. The decrease in viscosity of chitosan from acidic to alkaline pH values also indicated changes in the conformation of chitosan chains and the degree of entanglement. The amino groups of glucosamine residues are highly ionized (NH_3^+) at acidic conditions and the hydrodynamic size of chitosan chains is greater. However, at low polysaccharide concentration the effect of pH was less pronounced. In diluted solutions, polymer chains are isolated with no chain-chain interactions and their conformational changes may have less effect on the solution viscosity [23].

The viscosity decreased by increasing the NaCl concentration to 0.1 M of both polysaccharide solutions. This behavior was less evident at low concentration and at very high ionic strength (Fig. 2B). The greatest change was observed in chitosan solutions at 1%, where the viscosity was 172 mPa.s without NaCl and decreased to 110 mPa.s at 0.1 M NaCl.

The low effect of ionic strength in alginate solutions was probably related to the high residual Na^+ ions concentration coming from the sodium alginate dissociation in aqueous media. The viscosity of polyelectrolyte solutions is strongly affected by the ionic strength, since the dissolved ions in the solvent interact with chains causing charge screening, which in turn, induces the coiling of chains and reduces the degree of solvation [25].

3.3. Changes in the whiteness index of polysaccharide solutions

The whiteness index (WI) of polysaccharide solutions was used to determine the presence of insoluble aggregates, which may have an effect on the optical properties of nanolaminates. WI of alginate and chitosan solutions was evaluated as a function of pH, ionic strength and polysaccharide concentration (Fig. 3). Alginate solutions did not present significant differences in WI, neither by increasing the polysaccharide concentration nor by changing the pH of solutions (Fig. 3A). This suggests the absence of insoluble aggregates and solutions exhibited a clear appearance.

On the other hand, WI of chitosan solutions at acidic conditions (pH 3-5) was similar regardless the polysaccharide concentration, being translucent solutions. At pH values greater than 5, an abrupt increase could be appreciated and solutions were rather opaque. This is reasonable due to the presence of insoluble clumps that could be observed with the naked eye, which tend to scatter the light more strongly and increase the luminosity (L^*) of the solutions. This was attributed to the folding of chitosan molecules as the solution pH was near to the pK_a value (6.3 - 7.5), causing molecular aggregation and increased light scattering. Moreover, a further increase of the ionic strength did not cause changes in WI of both alginate and chitosan solutions, at least within the range of NaCl concentrations used in this work (Fig.3B). This confirmed that the polysaccharide solutions were physically stable in the presence of sodium ions.

3.4. Buildup mechanism of alginate/chitosan nanolaminates

Nanolaminates were assembled on quartz slides for the analysis of absorbance. The conditions of preparation of the adsorbing solutions were fixed, so that polysaccharides were equally charged at medium ionic strength. Therefore, nanolaminates were assembled using alginate and chitosan solutions at 0.5%, 0.2 M NaCl and pH 5 and 4, respectively. The high ionic strength can increase layer thickness of the assemblies [15]. Moreover, the formation of stable nanolaminates has been demonstrated when both polysaccharides have a similar charge density [26].

UV-visible spectra of five bilayers (alginate/chitosan) are shown in Fig. 4A. Absorbance increased as a function of the number of layers deposited. This behavior confirms the sequential formation of layers after an adsorption process. UV-visible spectroscopy is a practical and reliable technique that allows monitoring the buildup of nanolaminates by increases in the optical density [27], and although the mass adsorbed cannot be quantified, information about the growth regime of nanolaminates can be obtained.

The experimental conditions of the adsorbing solutions may affect the kinetic of adsorption of the polysaccharides, resulting in different growth regimes [28]. Therefore, the type of growth regime was evaluated by plotting the absorbance at 200 nm vs the number of layers. At this wavelength, alginate solutions present the maximum absorption peak, whereas chitosan solutions does not show adsorption within the UV-visible range (data not shown). Interestingly, alginate peak could not be observed in the nanolaminates spectra, probably due to a change in the molar absorptivity of the chromophore groups of alginate interacting with chitosan. In fact, it has been observed that nanolaminates composed by two polyelectrolytes can form molecular *blends* with intermediate spectrum [29].

The type of growth observed in alginate/chitosan nanolaminates was exponential, which is characterized by an increasing rate of mass deposition with each additional layer. This could be explained by the capacity of certain polyelectrolytes to diffuse in/out of the structure; this *free* chains can interact with oppositely-charged molecules of the absorbing solution [28,30]. Other authors have demonstrated that chitosan chains are able to diffuse vertically (out of the plane), interacting with oppositely-charged adsorbing species in the solution. This behavior was observed in chitosan/heparin assemblies [15].

It is also known that an increase in ionic strength of the adsorbing solutions results in exponential growth nanolaminates, since polyelectrolyte chains are deposited in a coiled conformation [31]. Therefore, the exponential growth of alginate/chitosan nanolaminates could be probably explained by the combined effect of high ionic strength and the diffusion of chitosan and not alginate in the structure of nanolaminates.

3.5. Surface ζ-potential

The surface ζ-potential of the nanolaminates is useful for monitoring changes in the electrical charge after a new layer formation. Surface ζ-potential values changed in terms of sign and magnitude of the electrical charge after a layer deposition (Fig. 5). Initially, the surface ζ-potential of the bare substrate (PET sheets) was 49 mV, and the first alginate layer led to a negative ζ-potential (≈ -32 mV). After the adsorption of the second chitosan layer, surface ζ-potentials changed to positive (≈ 52 mV). These results confirmed the charge reversal of the surface, which is the principle of the layer-by-layer technique. These results are in concordance with those previously reported for polypeptide-polysaccharide assemblies [32]. The charge inversion on the surface after a new layer has been observed also in layer-by-layer systems formed on spherical templates such as multilayer emulsions [33].

It is worth mentioning that the magnitude of surface ζ-potential values of chitosan layers (between 24 and 51 mV) were slightly superior to those observed in alginate layers (between -23 and -32 mV) although the initial electrical charge of both polysaccharides in solution were similar (ζ-potentials: -36 mV, alginate; 37 mV, chitosan). These differences might be related to different adsorption rates of both polysaccharides during the assembly of layers, or to the ability of chitosan free chains to diffuse toward the surface, probably increasing the surface ζ-potential. Another important factor influencing the surface electrical charge of nanolaminates is the ionic strength, since the coiled conformation adopted by polyelectrolytes favors a greater material deposition on the forming layer, which might also increase the magnitude of the electrical charge in the surface. These results are of great interest when designing nanolaminates for food applications, thus offering the possibility to control attractive or repulsive interactions between the coated food surface and other charged food ingredients.

3.6. Wetting properties

Wettability is one of the most important properties of solid surfaces and describes the ability of a liquid to spread over a certain surface, giving rise to a continuous film (spontaneous spreading) or discrete droplets (partial wetting). Interactions between a surface and a liquid depend on the free energies at the solid/liquid interface. The most common approach to discuss the wetting properties is through the contact angle. This parameter is governed by the competition between cohesion of a liquid to itself and adhesion of a liquid to a solid, this indicating the degree of hydrophilicity or hydrophobicity of the surface [34].

Water contact angles of nanolaminates created on PET were evaluated after a layer deposition (Fig. 6). The contact angle (θ) of bare PET was 85º, as reported by other authors [35]. After an alginate layer assembly, there was a decrease in θ to ≈52º that further increased to ≈70º with the subsequent deposition of a chitosan layer. These results are in concordance with other studies in alginate/polyethyleneimine and κ-carrageenan/chitosan nanolaminates that reported changes in the contact angle as a function of the number of layers [36]. Moreover, greater contact angle values were observed as the number of layers increased in nanolaminates, reaching θ of 14º in alginate layers and 75º in chitosan layers. Chitosan has more hydrophobic features than alginate, which has been attributed to the non-polar impurities contained in all commercial chitosan samples, rather than to the possible orientation of acetyl moieties at the solid/air interface [56]. These observations highlight the feasibility of the layer-by-layer technique as a strategy to modify the wetting properties of food surfaces, being interesting to design systems that can control the humidity of food products.

3.7. Thermal properties

DSC profiles of uncoated and coated substrate (PET sheets) by alginate/chitosan nanolaminates were examined (Fig. 8). In general, the presence of nanolaminates did not change the glass transition temperature (T_g) and the melting temperature (T_m) of the substrate. Probably, the mass ratio between PET and nanolaminates was too large, and hence the thermal properties of the composite material was governed by the PET. The results obtained in this study for the T_g and T_m of PET are in concordance with previous studies [37].

On the other hand, a slight increase in the enthalpy of melting (ΔH_m) was observed in coated PET by alginate/chitosan nanolaminates, compared to uncoated PET. This increase could be related with a barrier effect of nanolaminates against the gases generated during the polymer degradation, thus slowing down the process [38]. Another possibility is that the great accumulation of alginate and chitosan chains on the surface could increase in

polymer crystallinity, changing the enthalpy of melting, as suggested previously for alginate/chitosan nanolaminates assembled on PET [35].

3.8. Microstructure

The microstructure and topography of alginate/chitosan nanolaminates are presented in Fig. 8. Experimental parameters including pH, ionic strength, deposition time or temperature of polyelectrolyte solutions have an important impact on the final morphology of nanolaminates, originating different structures such as stratified or solid, as well as different degrees of porosity. In this study, nanolaminates exhibited a dense architecture, being difficult to detect the stratified inner layers. However, it was possible to estimate the average thickness, being around 700 nm for 10-layer assemblies. It has been reported that 20-layer nanolaminates growing exponentially can reach thicknesses > 10 μm, whereas assemblies with a linear growth are typically around 100 nm thick, having equal number of layers [39].

Other authors reported that thickness of exponential growing chitosan/hyaluronan assemblies containing 24 layers was about 6 μm thick [60]. The topography was characterized by the presence of big clusters connected in a net of polysaccharide chains, which could be attributed to the electrostatic interactions between alginate and chitosan molecules. These observations are in line with those reported previously about the topography of chitosan-grafted/alginate assemblies [40].

4. Conclusions

Food-grade alginate and chitosan were assembled into nanolaminates using the layer-by-layer technique. The analysis of the properties of polysaccharide solutions before deposition revealed changes in the ζ-potential, viscosity and whiteness index influenced by changes in the molecular conformation of polysaccharides under different conditions. From this study, it was found that the conditions where alginate and chitosan were physically stable, with a medium electrical charge at high ionic strength was 0.5%, 0.2 M NaCl and pH 5 and 4, respectively. The build-up of nanolaminates assembled under these experimental parameters could be confirmed by the absorbance increase of the substrate with an additional layer, and it presented an exponential growth regime induced by the ability of chitosan to diffuse throughout the structure and the adsorption of polysaccharides at high ionic strength. The surface ζ-potential of nanolaminate was affected by the type of polysaccharide in the terminal layer, being positive for chitosan layers and negative for alginate layers. Charge reversal on the surface also indicated that the assembly process was carried out successfully. The wetting properties of nanolaminates also

varied as a function of the number of layers, observing partially hydrophilic or hydrophobic surfaces when alginate or chitosan was the terminal layer, respectively. Regarding the thermal properties, no changes were observed in the thermal properties of the substrate coated by 10-layer assemblies. Results obtained from this study are relevant in the design of food-grade nanolaminates and get specific features, simply by controlling the experimental conditions. In addition, the information generated elucidates the great potential of nanolaminates made from food-grade materials as a strategy for modifying food surfaces or food contact materials, for example, inducing attractive or repulsive interactions between food ingredients, or controlling the moisture of a certain food surface.

5. Acknowledgments

This research was supported by the Ministerio de Ciencia e Innovación (Spain) (project AGL2009-11475). Author Acevedo-Fani also thanks to the University of Lleida for the pre-doctoral grant.

6. References

1. R. J. B. Peters, H. Bouwmeester, S. Gottardo, V. Amenta, M. Arena, P. Brandhoff, H. J. P. Marvin, A. Mech, F. B. Moniz, L. Q. Pesudo, H. Rauscher, R. Schoonjans, A. K. Undas, M. V. Vettori, S. Weigel, and K. Aschberger, Trends in Food Science & Technology **54**, 155 (2016).

2. J. Weiss, P. Takhistov, and D. J. McClements, Journal of Food Science **71**, R107 (2006).

3. J. Borges and J. F. Mano, Chemical Reviews **114**, 8883 (2014).

4. M. A. Cerqueira, A. C. Pinheiro, H. D. Silva, P. E. Ramos, M. A. Azevedo, M. L. Flores-López, M. C. Rivera, A. I. Bourbon, Ó. L. Ramos, and A. A. Vicente, Food Engineering Reviews **6**, 1 (2014).

5. L. Mao and S. Miao, Food Engineering Reviews **7**, 439 (2015).

6. O. Benjamin, P. Silcock, J. Beauchamp, A. Buettner, and D. W. Everett, Food Chemistry **140**, 124 (2013).

7. M. L. Flores-López, M. A. Cerqueira, D. J. de Rodríguez, and A. A. Vicente, Food Engineering Reviews **8**, 292 (2016).

8. A. Ferreira, V. Alves, and I. Coelhoso, Membranes **6**, 22 (2016).

9. T. Crouzier, T. Boudou, and C. Picart, Current Opinion in Colloid & Interface Science **15**, 417 (2010).

10. K. I. Draget, S. T. Moe, G. Skjak-Braek, and O. Smidsrod, in Food Polysaccharides and Their Applications, edited by A. M. Stephen, G. O. Phillips, and P. A. Williams (CRC Press. Taylor & Francis Group, Boca Ratón, FL, 2006), pp. 289–334.

11. G. O. Phillips and P. A. Williams, Handbook of Hydrocolloids, 2nd edn (Woodhead Pub, 2009).

12. American Chemistry Council, Plastics 1 (2013).

13. W. Graisuwan, O. Wiarachai, C. Ananthanawat, S. Puthong, S. Soogarun, S. Kiatkamjornwong, and V. P. Hoven, Journal of Colloid and Interface Science **376**, 177 (2012).

14. H.-Y. Zhang, A.-J. Miao, and M. Jiang, Materials Chemistry and Physics **141**, 482 (2013).

15. M. Lundin, F. Solaqa, E. Thormann, L. MacAkova, and E. Blomberg, Langmuir **27**, 7537 (2011).

16. L. Salvia-Trujillo, M. A. Rojas-Graü, R. C. Soliva-Fortuny, and O. Martín-Belloso, Food Hydrocolloids **30**, 401 (2013).

17. A. Acevedo-Fani, L. Salvia-Trujillo, R. Soliva-Fortuny, and O. Martín-Belloso, Biomacromolecules **16**, 2895 (2015).

18. K. I. Draget, in Handbook of Hydrocolloids, edited by G. O. Phillips and P. A. Williams, Second (CRC Press and Woodhead Publishing, Boca Ratón, FL, 2009), pp. 807–825.

19. M. G. Carneiro-da-Cunha, M. A. Cerqueira, B. W. S. Souza, J. A. Teixeira, and A. A. Vicente, Carbohydrate Polymers **85**, 522 (2011).

20. A. Abodinar, A. M. Smith, and G. A. Morris, Carbohydrate Polymers **112**, 6 (2014).

21. X. He, F. Meng, A. Lin, J. Li, and C. Y. Tang, AIChE Journal **62**, 2501 (2016).

22. P. Zhang, J. Qian, Q. An, B. Du, X. Liu, and Q. Zhao, Langmuir **24**, 2110 (2008).

23. D. L. B. Wetzel and G. Charalambous, Instrumental Methods in Food and Beverage Analysis (Elsevier, 1998).

24. J. Milani and G. Maleki, in Food Industrial Processes–Methods and Equipment, edited by B. Valdez (InTech, 2012), pp. 17–38.

25. S. Morariu, C. E. Brunchi, and M. Bercea, Industrial & Engineering Chemistry Research **51**, 12959 (2012).

440 26. T. Radeva, K. Kamburova, and I. Petkanchin, Journal of Colloid and Interface Science **298**, 59 (2006).

441 27. D. T. Haynie, L. Zhang, J. S. Rudra, W. Zhao, Y. Zhong, and N. Palath, Biomacromolecules **6**, 2895 (2005).

442 28. P. Bieker and M. Schönhoff, Macromolecules **43**, 5052 (2010).

443 29. P. Lavalle, J.-C. Voegel, D. Vautier, B. Senger, P. Schaaf, and V. Ball, Advanced Materials (Deerfield Beach,
444 Fla.) **23**, 1191 (2011).

445 30. C. Picart, J. Mutterer, L. Richert, Y. Luo, G. D. Prestwich, P. Schaaf, J. C. Voegel, and P. Lavalle, Proceedings
446 of the National Academy of Sciences of the United States of America **99**, 12531 (2002).

447 31. S. Boddohi, C. E. Killingsworth, and M. J. Kipper, Biomacromolecules **9**, 2021 (2008).

448 32. C. Picart, P. Lavalle, P. Hubert, F. J. G. Cuisinier, G. Decher, P. Schaaf, and J.-C. Voegel, Langmuir **17**, 7414
449 (2001).

450 33. F. Liu, D. Wang, C. Sun, D. J. McClements, and Y. Gao, Food Chemistry **205**, 129 (2016).

451 34. E. M. Baba, C. E. Cansoy, and E. O. Zayim, Applied Surface Science **350**, 115 (2015).

452 35. M. G. Carneiro-da-Cunha, M. A. Cerqueira, B. W. S. Souza, S. Carvalho, M. A. C. C. Quintas, J. A. Teixeira,
453 and A. A. Vicente, Carbohydrate Polymers **82**, 153 (2010).

454 36. B. G. de S. Medeiros, A. C. Pinheiro, M. G. Carneiro-da-Cunha, and A. A. Vicente, Journal of Food
455 Engineering **110**, 457 (2012).

456 37. C. A. Grant, A. Alfouzan, T. Gough, P. C. Twigg, and P. D. Coates, Micron (Oxford, England : 1993) **44**, 174
457 (2013).

458 38. Z. Ayhan, S. Cimmino, O. Esturk, D. Duraccio, M. Pezzuto, and C. Silvestre, Packaging Technology and
459 Science **28**, 589 (2015).

460 39. G. V. Martins, J. F. Mano, and N. M. Alves, Nanostructured Self-Assembled Films Containing Chitosan
461 Fabricated at Neutral pH (2010).

462 40. G. V Martins, J. F. Mano, and N. M. Alves, Langmuir **27**, 8415 (2011).

463

Figure 1. Influence of (**A**) pH and (**B**) NaCl concentration on ζ-potential of alginate (ALG) and chitosan (CHI) solutions at different concentrations. The pH of biopolymer solutions with NaCl was 5 and 4, respectively.

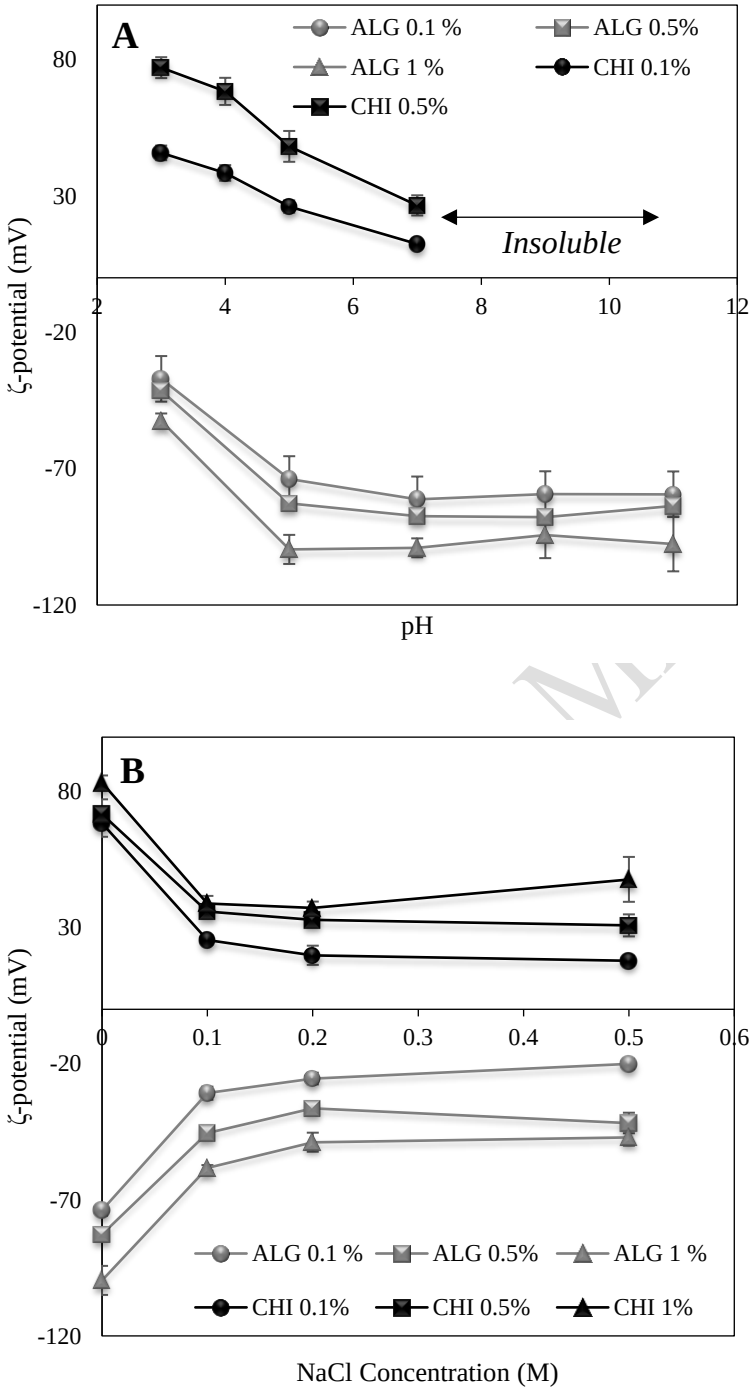

Figure 2. Influence of pH (**A**) and (**B**) NaCl concentration on apparent viscosity of alginate (ALG) and chitosan (CHI) solutions at different concentrations. The pH of biopolymer solutions with NaCl was set to 5 and 4, respectively.

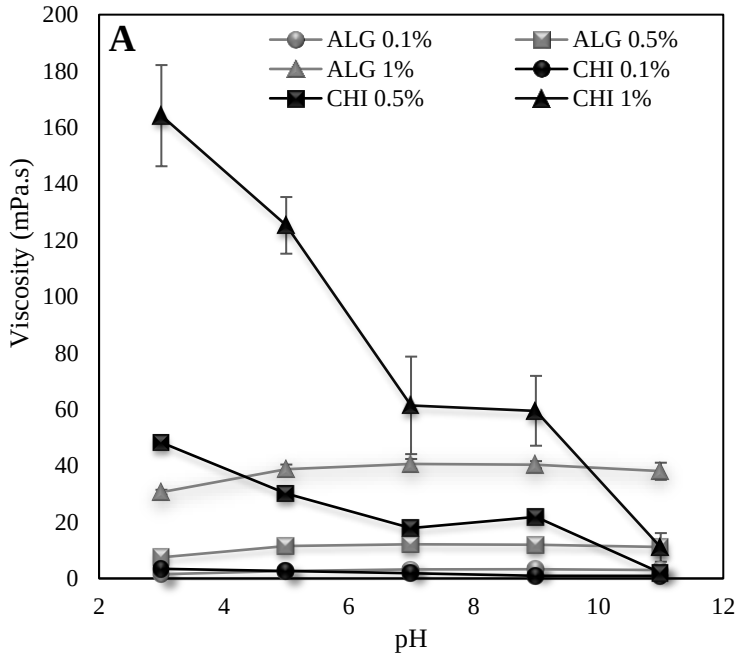

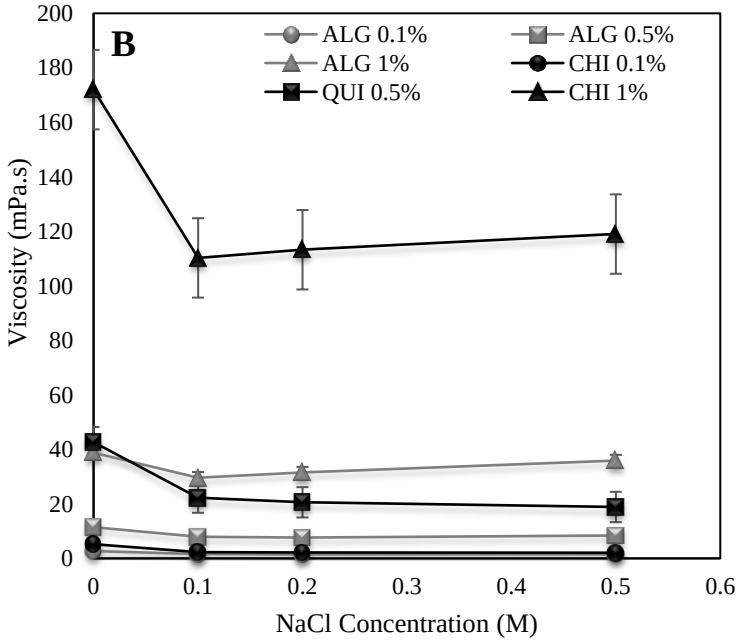

Figure 3. Effect of (**A**) pH and (**B**) NaCl concentration on whiteness index of alginate (ALG) and chitosan (CHI) solutions at different concentrations. The pH of biopolymer solutions with NaCl was set to 5 and 4, respectively.

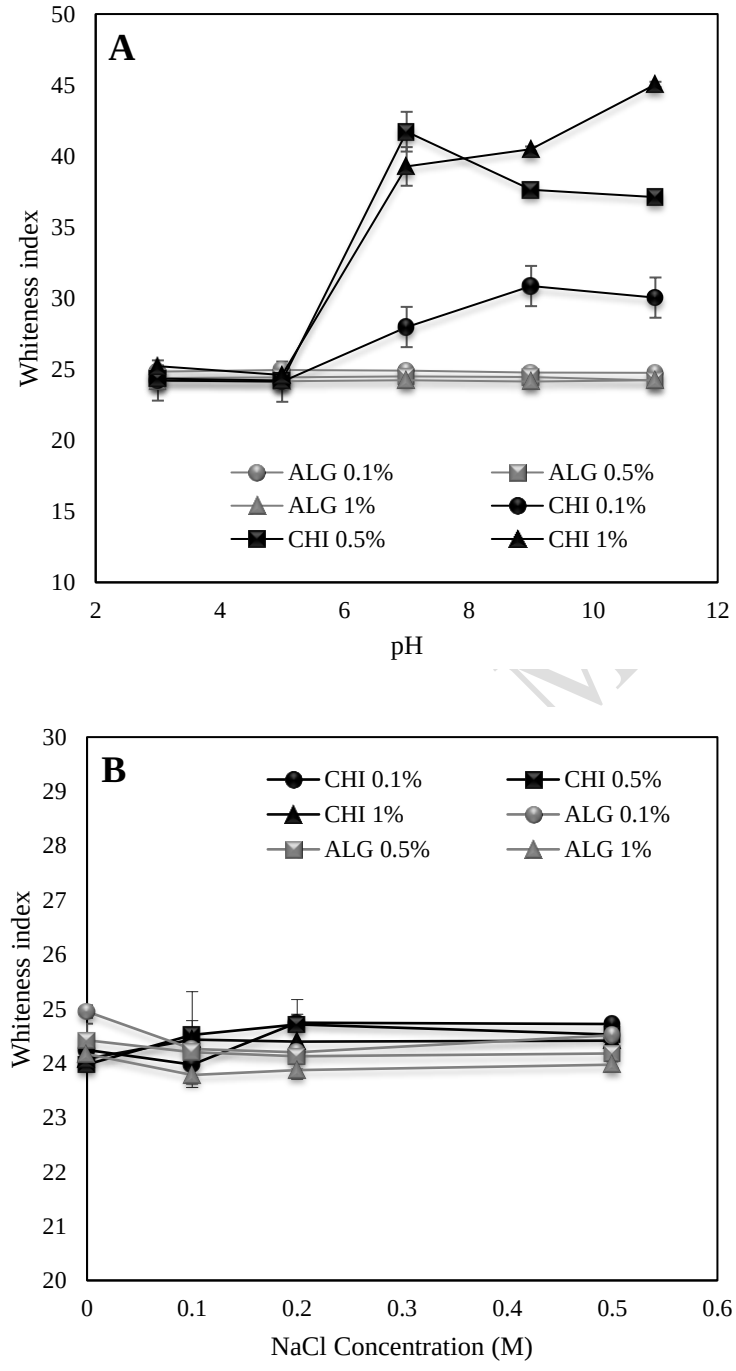

Figure 4. (A) UV-visible spectra and (B) Absorbance at 200 nm as a function of layers (L) deposited. Nanolaminates were obtained from alginate and chitosan 0.5 % (w/w), 0.2 M NaCl and pH 5 and 4, respectively.

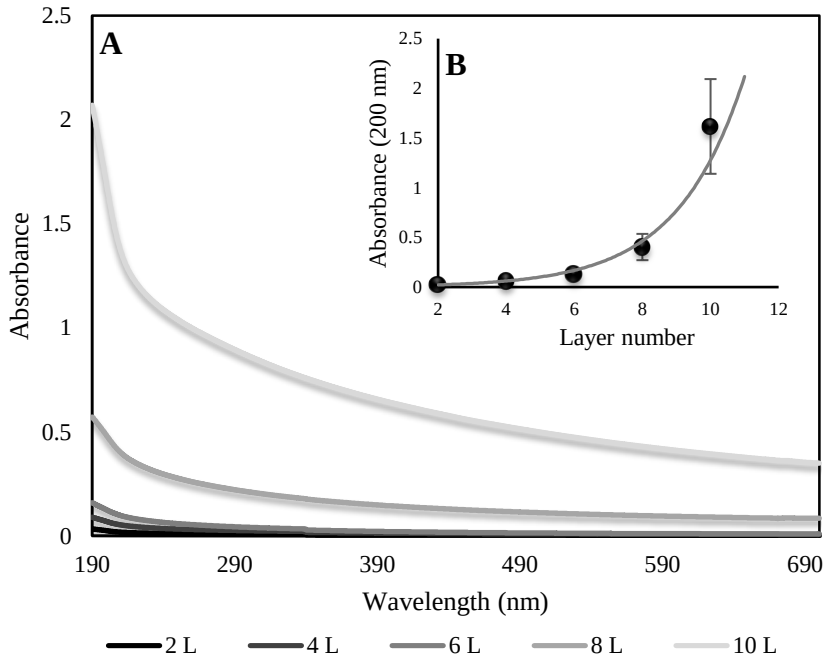

Figure 5. Surface ζ-potentials as a function of the number of alginate (ALG) and chitosan (CHI) layers deposited in a nanolaminate system. ALG and CHI were prepared at 0.5 % (w/v), 0.2 M NaCl and pH 5 and 4, respectively.

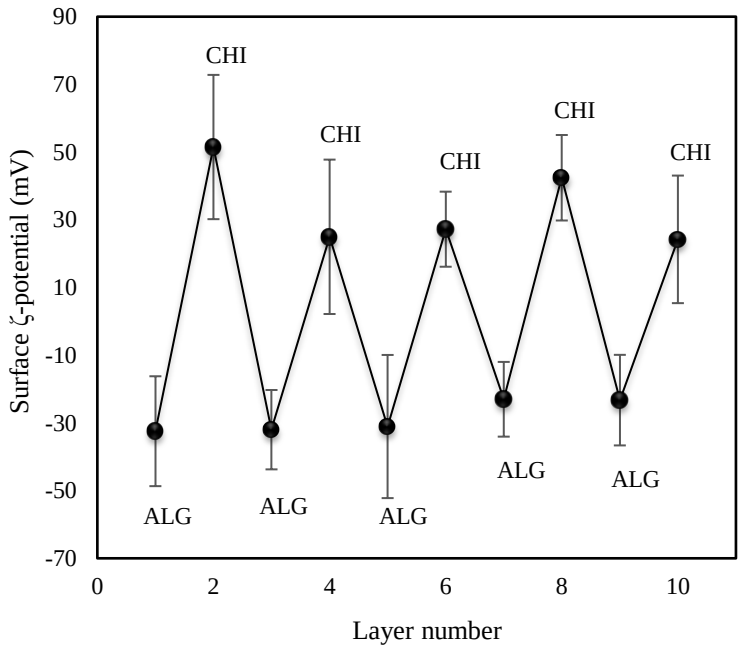

Figure 6. Water contact angles of the surface of nanolaminates as a function of the number of alginate (ALG) and chitosan (CHI) layers. ALG and CHI solutions were prepared at 0.5 % (w/v), 0.2 M NaCl and pH 5 and 4, respectively.

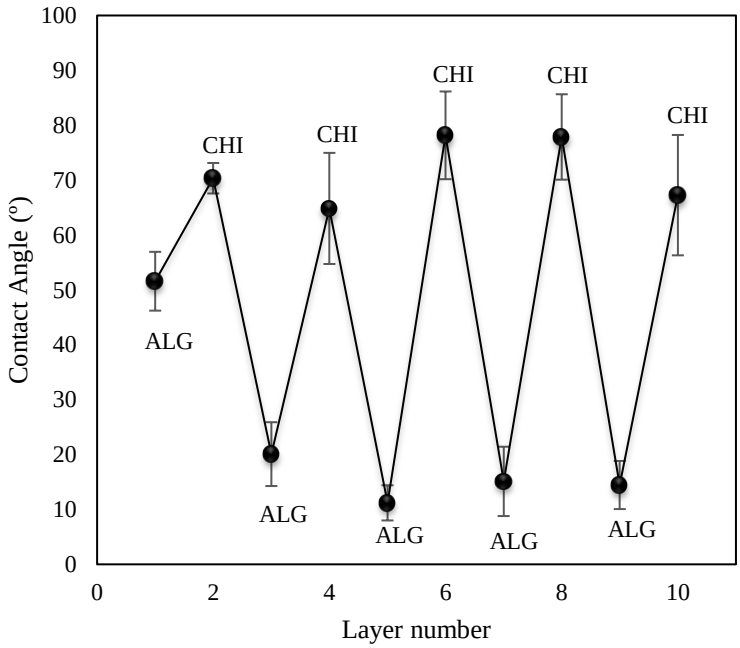

Figure 7. DSC profile of bare PET and PET containing alginate/chitosan nanolaminates.

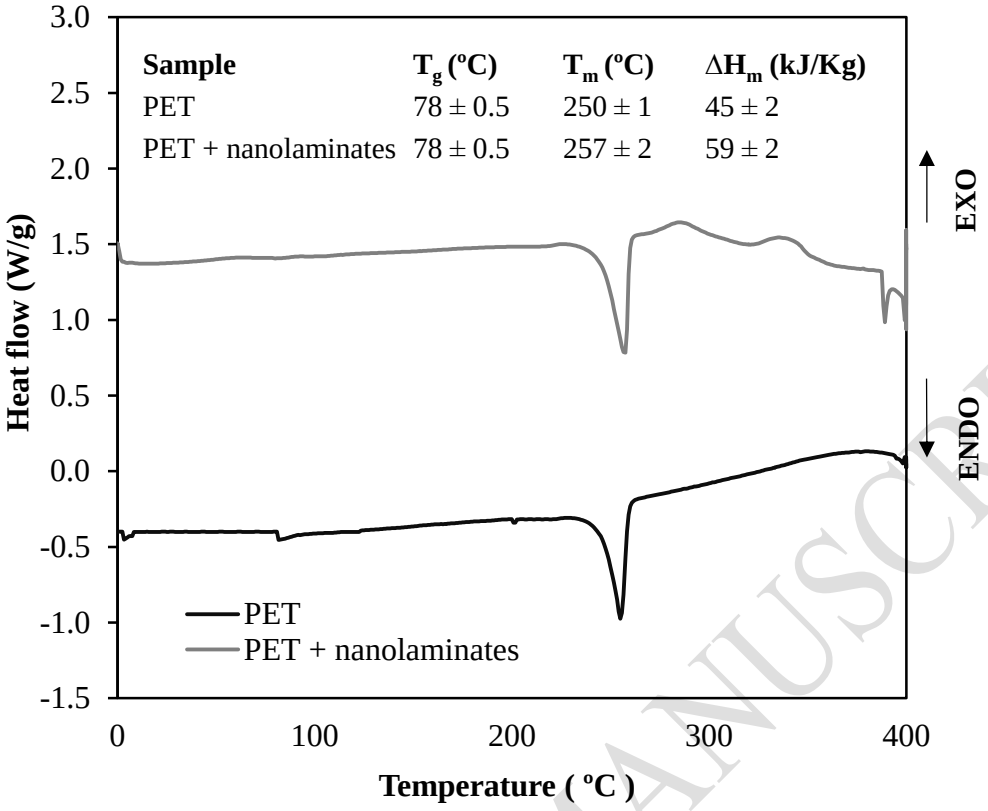

Figure 8. Microstructure and surface of alginate/chitosan nanolaminate examined by SEM microscopy.